Journal of Optoelectronics and Advanced Materials Vol. 7, No. 5, October 2005, p. 2693 - 2706

STRUCTURAL AND ELECTRICAL PROPERTIES OF UNDOPED SnO_2 FILMS DEVELOPED BY A LOW COST CVD TECHNIQUE WITH TWO DIFFERENT METHODS: COMPARATIVE STUDY

N. D. Papadopoulos, P. E. Tsakiridis, E. Hristoforou*

Laboratory of Physical Metallurgy, School of Mining and Metallurgical Engineering National Technical University of Athens 9, Iroon Polytechniou Street, 157 80 Zografou, Athens, Greece

Uniform, conductive SnO_2 thin films have been developed by a low – cost CVD technique using a simple, home-made setup. Two methods with different sources of oxygen were applied. The thin layers were deposited on glass substrates. Stannic chloride was used as the precursor and the substrate temperature varied from 485 to 545 ^oC. The microstructure and the surface morphology of the produced films were examined by X-Ray Diffraction and scanning electron microscopy, with EDAX analysis. The films were found to be polycrystalline, presenting a preferred orientation along the (110) plane. Thickness of films varied from 150 nm to 400 nm. Extended study of the mechanism of diffusion of sodium ions out of the glass as well as its effects on film's quality was carried. Crystals of NaCl formed on the matrix of films, which had been grown with air functioning as the oxidizer. Measurements of the mean surface's roughness were conducted by a profilometer. When pure oxygen was used, the produced films presented a smoother surface without any pinholes or undesirable crystal formation. Electrical resistivity at room temperature and in the range from 25 to 250 ^oC was also measured. Films of high conductivity were obtained for both methods at deposition temperatures between 515 and 545 ^oC. For films of high crystallinity grain scattering and scattering from ionised impurities are the major factors influencing conductivity. When air is used as the oxidizer, films develop fully at higher deposition temperatures. In this case however, oxidation diminishes vacancies, which are present at a high degree since the oxygen concentration in air is low. In both methods, annealing in air improved the film crystallinity and conductivity.

(Received June 28, 2005; accepted September 22, 2005)

Keywords: CVD, Thin films, Tin oxide, Oxidizer, Characterization

1. Introduction

Several kinds of materials, such as tin oxide, indium tin oxide (ITO), and zinc oxide, are known as Transparent Conductive Oxides (TCO). From these materials, tin oxide shows unique characteristics in chemical inertness, stability to heat treatment and mechanical hardness [1].

Thin films of SnO_2 are currently being used in a wide range of applications, e.g. electrodes in electroluminiscent displays, protective coatings, gas and chemical sensors [2,4], touch-sensitive switches [5] and many others [6-8], mainly due to their outstanding properties [6, 9]. Such films can be prepared by various methods, such as reactive sputtering [10, 11], spray – pyrolysis, sol – gel, vacuum evaporation and chemical vapor deposition (CVD), using either organic or inorganic precursors [5]. It has been extensively reported that the variety of preparation methods has led to the thin films having different structural and electrical properties. The latter are critically influenced by oxygen vacancies serving as donors in tin oxide films. In principle physical methods such as sputtering and thermal evaporation lead to weakly non-stoichiometric tin oxide with co-existence of

* Corresponding author: eh@metal.ntua.gr

other insulating phases like SnO [6], resulting into relatively high resistive films. On the other hand, chemical methods lead to strongly non-stoichiometric tin oxide, resulting into comparatively low resistive films [2, 7].

CVD remains the most widely used deposition technique in many fields, especially for depositing thin films of electronic materials. It is capable of producing highly dense films with good adhesion to the substrate. It can be used to uniformly coat complex shaped components and deposit films with excellent conformal coverage. Such distinctive feature outweighs the PVD process [11, 12].

However, CVD-based methods generally involve complex chemistry and chemical process, which include the nature of chemical precursors, toxic or corrosive byproducts, chemical reactions in the gas phase and heterogeneous reactions. This is why these methods demand often a sophisticated equipment to control adequately the CVD process parameters. In this case though, the cost is relatively high [11].

The present research work aimed at the production of uniform, conductive undoped SnO_2 thin films by a low – cost CVD technique, using $SnCl_4 \cdot 5H_2O$ as the precursor, through the aid of a conventional thermal CVD system. Teflon, instead of stainless steel was used extensively. A simple system at the end of the experimental setup was applied, in order for the byproducts to be neutralized. Thin films of SnO_2 were produced according to two different methods. In the first one, atmospheric air produced by an air compressor functioned both as the carrier gas and as the source of oxygen, whereas in the second method argon served as the carrier gas and oxygen of high purity (99,9999 %) as the oxidizer. In terms of total cost, the first method is more economical. The variables studied were:

- The substrate temperature
- The exit pressure of the air compressor, namely the pressure of the incoming precursor's vapors (first method)
- The Argon flow (second method)
- The deposition duration

2. Experimental

Tin oxide films were deposited on amorphous glass substrates through the following reaction:

$$SnCl_4 + O_2 \rightarrow SnO_2 + 2\ Cl_2 \quad (1)$$

Common soda-lime sheet glasses of 1.1 mm thickness were used as substrates. The films were grown in a hot wall horizontal reactor, constructed in the laboratory of Physical Metallurgy of the National Technical University of Athens, by oxidation of $SnCl_4$ vapors. The reactor chamber was constructed by resistance-heated quartz and had a circular section. The glass substrates (2cm x 1 ½ cm) were placed on a graphite susceptor. A slightly inclined aluminum base, which served as a source of extra support, was used mainly because this inclination is known to provide the best conditions for laminar flow [11-13]. This base could withstand thermal oxidation. The temperature was controlled by a quartz-sheathed alumel-chromel thermocouple embedded within the supportive base and held within an accuracy of ± 5°C. The precursor was contained in glass bubbler and the nozzle to the substrate had a distance of 50 cm. The substrate temperature was varied from 485 °C to 575 °C in steps of 30 °C. Two plugs, made of Teflon, were used at the edges of the chamber, so as to seal off the interior space. At the exit plug a pressure gauge was adjusted. Furthermore, on each plug two manual valves allowed the transport of the gaseous materials in and out of the chamber, via the corresponding carrier line. All carrier lines were also made of Teflon.

The deposition started with the introduction of the precursor's vapors into the air stream. After deposition, the samples were allowed to cool down to temperatures in the order of 80 – 90 °C in the same air stream as for the deposition. This process (which further enhanced the oxidation) lasted several minutes emphasizing the fact that the higher the deposition temperature, the longer the cooling period.

The by-products of the reaction (1) were led into two polypropylene tanks, which contained diluted NaOH 3 M. By this arrangement the gaseous Cl_2 was neutralized before reaching the system's exit. A mechanical pump at the end of the whole system was implemented, so as to absorb the by-products that had not been neutralized. Mechanical valves for the pumped air adjustment and an extra carrier line were also used for safety reasons. The experimental setup for the second method is shown in Fig. 1. By comparing the setups of methods one and two, it is evident that the only difference between them is the system input.

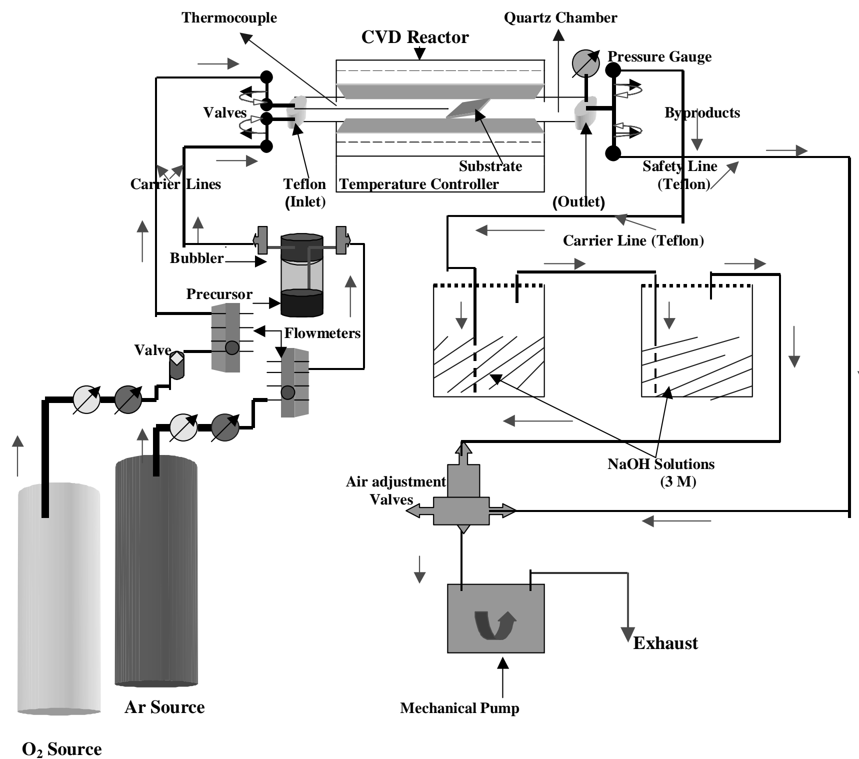

Fig. 1. Experimental setup for the development of undoped SnO_2 films.

The deposition parameters studied are given in Table 1. When atmospheric air was used as the oxidizer, the films prepared at 485, 515, 545 and 575 ^{o}C were denoted by D1, D2, D3 and D4. On the other hand, when pure oxygen was used, the films prepared at 485, 515, and 545 ^{o}C were denoted by P1, P2-P3, and P4-P5-P6, respectively. In this case the oxygen flowrate was kept constant during the process at 270 ml/min. Concerning the experiments conducted by the first method, the pressure values refer to the pressure with which the precursors were transferred into the reactor and not to the total pressure in its interior space.

The mineralogical phases and the mean grain size of the produced films were determined by X-ray diffraction (XRD) using a Siemens D5000 diffractometer with nickel-filtered $CuK\alpha_1$ radiation (=1.5405 A), 40 kV and 30 mA. The surface morphology was studied with the aid of a Jeol 6100 Scanning Electron Microscope (SEM). The chemical composition of the produced films was examined by a Noran TS 5500 Electron Dispersive Spectrometer (EDS) connected to the SEM. Measurements of the films' surface roughness were taken by a Dektak IIA profilometer. Film resistivity values were obtained by measuring the electrical resistance (R) at room temperature and at elevating temperatures. The thickness of the films varied from 150 nm to 400 nm. It was indirectly estimated by measuring the tiny step formation, which was produced when a second wafer

was placed over the half of the initial wafer's surface, on which deposition took place. This indirect measurement was taken via the same device used for roughness' measurements.

Table 1. Deposition conditions.

Sample Name	*Temperature (^oC)*	*Flowrate of carrier gas (std. ml/min)*	*Exit Pressure (bar)*	*Duration of deposition (min)*
D1	485		1.0	15
D2	515		1.0	15
D3	545		1.0	15
D4	575		1.5	10
P1	485	300		20
P2	515	300		20
P3	515	400		20
P4	545	400		15
P5	545	300		20
P6	545	400		20

3. Results and discussion

3.1 Mineralogical analysis of the deposited films by x-ray diffraction

XRD analysis of the as deposited tin oxide films confirmed that these were polycrystalline with tetragonal cassiterite (rutile type) structure. Other phases like α-SnO, β-SnO, Sn_2O_3, Sn_3O_4, etc. were not observed. The diffraction data was collected with 0.025 step width, over a 2θ range from 20° to 80°.

In all cases the preferred crystal face orientation of the undoped SnO_2 thin films was (110). Other planes corresponding to (111), (101), (200), (211), (220), (221), (301) and (321) also appeared with weaker intensities. In the case of sample D3 however, the (111) peak seemed to be the dominating one (Fig. 2a). Nevertheless, it should be noted that this specific orientation had been enhanced through the overlap, which occurred between the (111) peak and the (200) peak, which in turn was attributed to the presence of NaCl. In general, in CVD processes crystals of NaCl are often formed by the combination of the diffused out of the glass sodium ions with the chlorine ions of a metal-chloride precursor. The best way of minimizing this occurrence is the deposition of a thin layer of SiO_2, which acts as a migration barrier.

It was found that films exhibited higher crystallinity when air rather than pure oxygen was used as the oxidizer at the same deposition temperature. However, this is probably due to the higher deposition rate of the first method since the flowrate of air was significantly higher than the total sum of the flowrates of argon and oxygen, which were used for the second method. The lower rate of the precursor's flow in the second method could be the reason for the absence of peaks corresponding to NaCl since the film's surface roughness, which in high values accelerates the formation of NaCl crystals [14], was minimized during crystal growth.

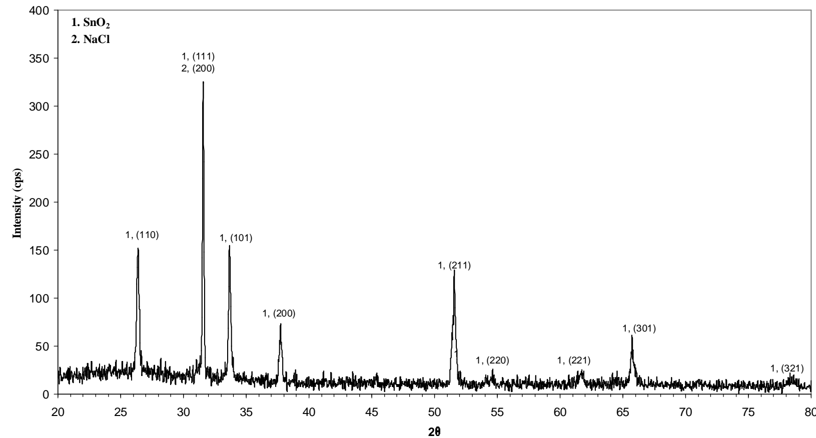

(a): Sample D3

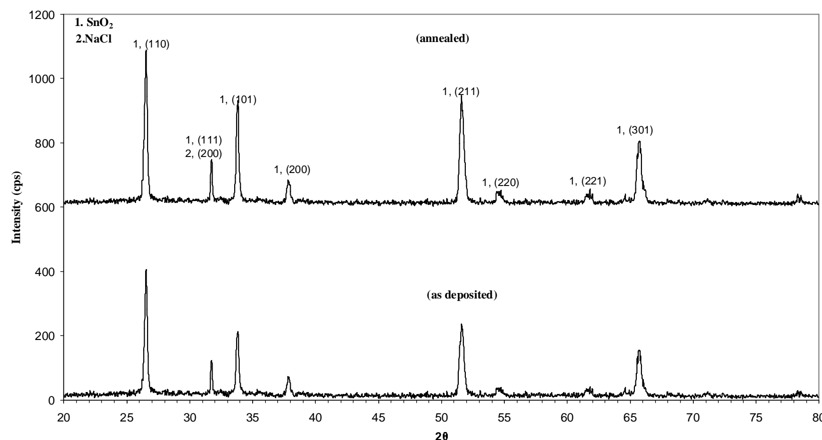

(b): Sample D4

Fig. 2. XRD analysis of undoped SnO_2 films produced by oxidation of $SnCl_4$ vapors with air with different deposition parameters on glass substrates and effect of post heat treatment on the crystallinity of sample D4.

It has been also observed that for both methods the increase of the deposition temperature favors the crystallinity of the film. By the increase of the deposition temperature, the mobility of the carriers also increases and, as a result, the rate of nucleation at different sites of lower free energy of the substrate becomes higher [15]. Moreover, it was concluded that the temperature was more of an influence on the crystallinity of films than the duration of deposition within the range investigated.

To investigate the effect of post deposition heat treatment in the crystallinity of SnO_2 films, annealing of various films took place at 580 ^oC for 30 min, in air. The XRD analysis of samples D4 and P5 before and after the heat treatment is given in Figs. 2b and 3b, respectively. It can be observed that the peak intensities increased further. The above observation could be explained by the fact that smaller crystallites generally have surfaces with sharper convexity. This provides a larger area of contact between adjacent crystallites, facilitating a coalescence process during the heat treatment to form larger crystallites [16]. What is more, annealing seems to play a critical role in the crystallinity of films when pure oxygen is used as the oxidizer. Specifically, in the case of sample P5 the crystallinity has increased by more than two orders of magnitude. The reason may be the complex mechanism of the absorbed species' reaction on the substrate's surface, which sometimes

leads to a less crystalline structure when a carrier gas different from the oxidizer is used. After annealing the film grows upon the crystalline structure of SnO_2 more easily.

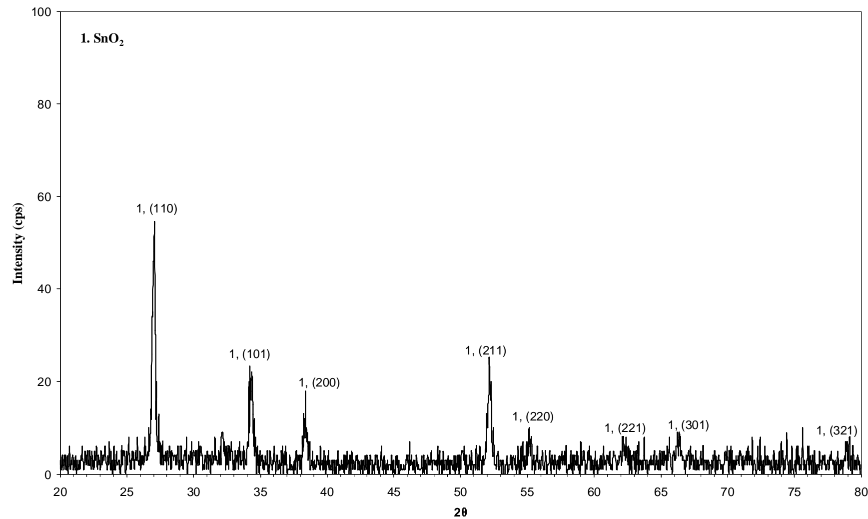

(a): Sample P3

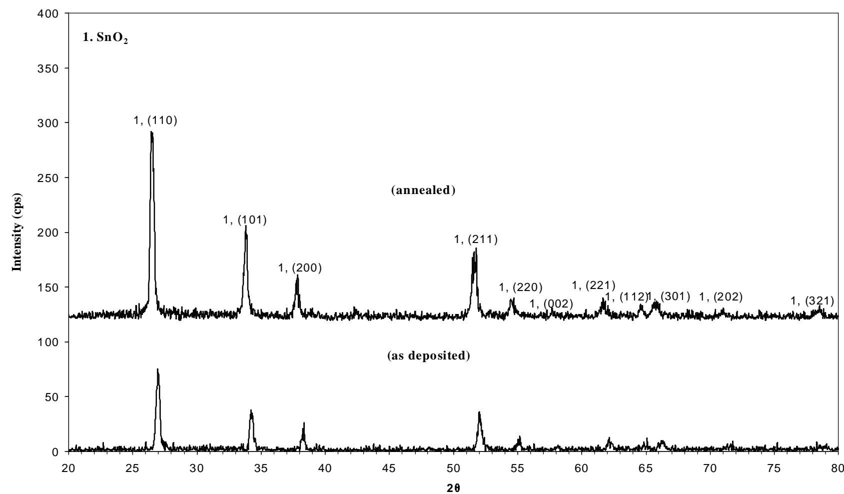

(b): Sample P5

Fig. 3. XRD analysis of undoped SnO_2 films produced by oxidation of $SnCl_4$ vapors with pure oxygen with different deposition parameters on glass substrates and effect of post heat treatment on the crystallinity of sample P5.

The mean grain size was determined from the full width at half maximum of the main peak using the classical Debye-Scherrer formula. The calculated values of crystallite size for all samples are given in Table 3. It is clear that through the increase of deposition temperature the rate of nucleation also rises. The end result is the subsequent increase of the mean grain size.

3.2 Examination of the deposited films' microstructure by SEM

The SEM micrographs of the films derived from the first method are given in Fig. 4 a-d. It can be observed that sample D1 is characterized by a lack of uniformity, especially at the edge of the substrate. SnO_2 film seems to not have fully grown mainly because of the short duration of deposition and the lower formation temperature. Sample D2 has grown with a porous

microstructure. The analysis of a pin-hole inside the film's mass (spot analysis) is given in Table 2 (EDAX analysis). According to the results it can be concluded that these holes do not end exactly at the substrate's surface. The %wt high concentrations of Sn and Na imply that an extremely thin film was formed previously. This ultra thin film probably exists as a mixed phase between SnO_2 and Na, at the exact interface between the substrate and the main as deposited film. Furthermore, the % wt high concentration of Si and Na proves that the latter really diffused out of the glass substrate.

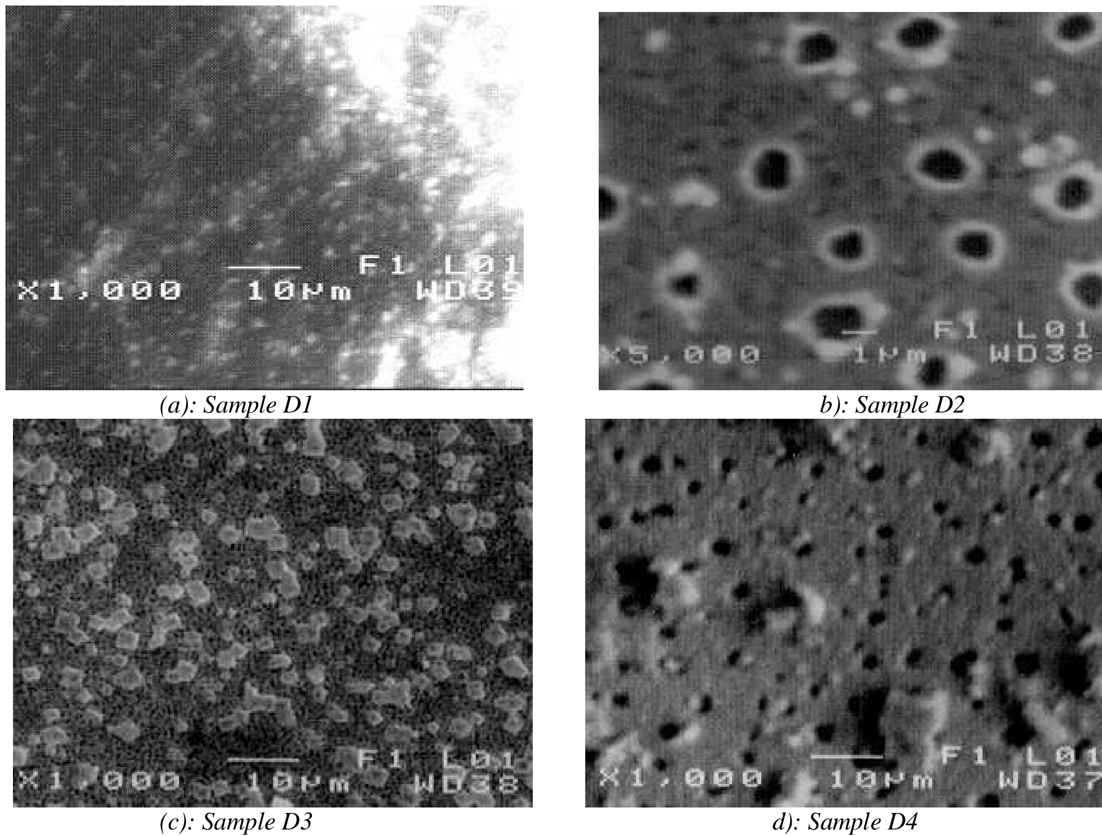

(a): Sample D1 *b): Sample D2*

(c): Sample D3 *d): Sample D4*

Fig. 4. Scanning Electron Microscopy micrographs. Samples D1-D4.

Table 2. EDAX Analysis.

Sample Name	*%wt O_2*	*%wt Sn*	*%wt Na*	*% wt Cl*	*%wt Si*
D1	56.83	34.16	0.42	1.97	6.62
D2	58.44	38.65	0.88	0.91	1.12
D2 (pin hole)	53.35	29.70	6.83	0.21	9.91
D3	59.40	37.01	1.45	1.57	0.57
D3 (crystal on matrix)	32.76	19.03	28.04	20.17	-
D4	59.98	35.47	2.26	1.85	0.44
P1	58.69	34.18	-	-	7.13
P2	59.67	39.16	0.32	0.21	0.64
P3	60.22	38.74	0.40	0.38	0.26
P4	60.60	38.32	0.58	0.36	0.14
P5	60.68	36.91	0.81	0.67	0.93
P6	60.77	37.89	0.61	0.54	0.19

For samples D1-D4 the O/Sn ratio was about 1.5 to 1.8. All samples contain Cl^- ion contamination. This was due to the concentration of Cl^- ions contained in the precursor. It was also observed that with the increase of substrate temperature the %wt concentration of Na^+ ions increases too. This indicates that the mechanism of Na^+ diffusion out of the glass is further activated by the increase in temperature [17]. As a result, the produced pores multiply at an accelerated rate as the deposition temperature increases. Particularly, in the case of sample D4, the above-mentioned process has severe effects on the film's surface. The size of the pores produced by diffusion was dramatically grown giving the film relatively poor properties.

Furthermore, in both cases of samples D3 and D4 crystals of NaCl can be well distinguished, with the former also having a smoother surface. These crystals have formed on the matrix of the films by diffusion of sodium ions and exist as a mixed phase between SnO_2 - NaCl. %wt concentrations of a typical NaCl crystal (sample D3) have been measured by an EDAX analysis (Table 2). The presence of NaCl crystals can also affect the microstructure of the SnO_2 thin films. In Fig. 5 it is shown that SnO_2 can develop in the dendritic form (sample D4). This occurrence was explained by the presence of NaCl crystals, which were "trapped" in the dendrites of SnO_2.

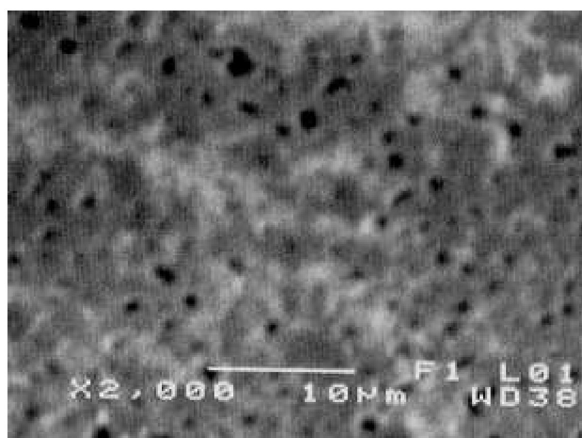

Fig. 5. Scanning Electron Microscopy micrograph of sample D4. Growth of SnO_2 in the dendritic form.

For samples grown according to the second method the O/Sn ratio was about 1.5 to 1.7. Concerning the SEM for films P1-P6 (Fig. 6) it is obvious that sample P1 has a quite smooth surface. However, it is very thin and that is probably the reason why it exhibits a high %wt concentration of Si. Sample P3 has grown highly uniform. Individual equiaxed crystallites with rounded grown features can be clearly seen. For sample P2 the temperature and the duration of deposition was the same as for P3. The former one, however, presents a much smoother surface, since the flowrate of the precursor was in this case lower.

At 545 ^oC three films with different deposition parameters were studied. All of them present a quite dense and uniform structure. As well as having a smooth surface, sample P4 was also grown with excellent step coverage. Sample P6, which was deposited with the maximum flow of the precursor presents a relatively high degree of surface roughness. The mean grain size in this case seems to have significantly increased. On the matrix of film P5 a few small crystals, probably of NaCl, have formed. As can be seen from the results of EDAX analysis (Table 2) all films contain Na and Cl ion contamination. However, the degree of this contamination is slightly lower for films P1-P6. This is why XRD analysis did not identify NaCl formation in the previous films as a definite mineralogical phase.

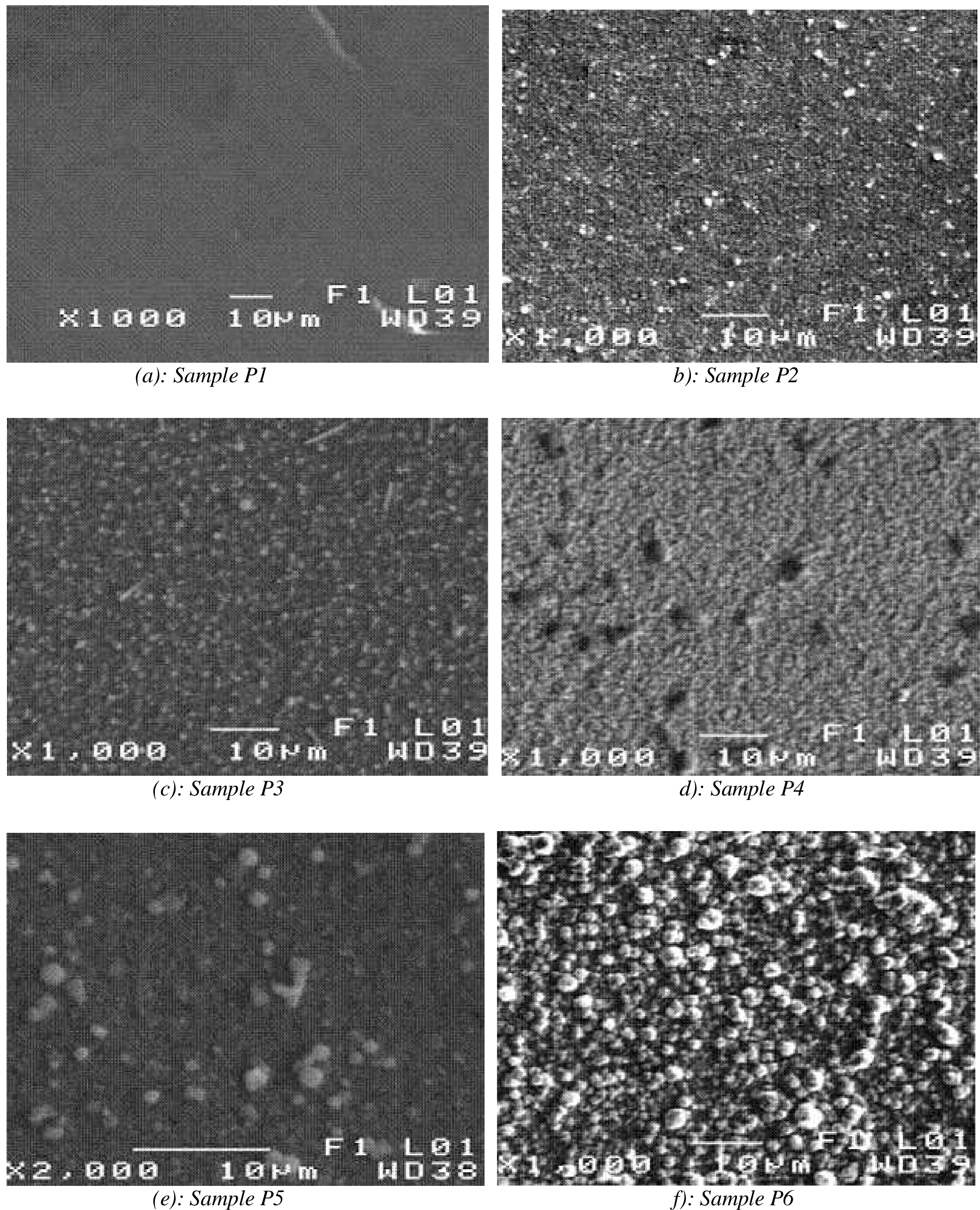

(a): Sample P1 *b): Sample P2*

(c): Sample P3 *d): Sample P4*

(e): Sample P5 *f): Sample P6*

Fig. 6. Scanning Electron Microscopy micrographs. Samples P1-P6.

3.3 Films' thickness and mean surface roughness

The differences in films' surface roughness values can be attributed primarily to the differences in film thickness. In general, the higher the total film thickness, the higher the surface roughness [14]. The different RMS values together with each film's thickness are given in Table 3. Fig. 7 shows the impact that increasing temperature has on film thickness, when the total precursor's quantity was kept constant. In the present study, the total precursor's quantity can be well defined either as the product of *P* (pressure with which the initial substances were transferred into the reactor

– first method) or as the product of $F_{c.g.}$ (flowrate of the carrier gas – second method) (by *t* (duration of deposition). In both cases the film thickness is almost in linear proportion to the deposition temperature. This is due to the fact that crystal growth and, consequently, the film's thickness increases with the increase of temperature.

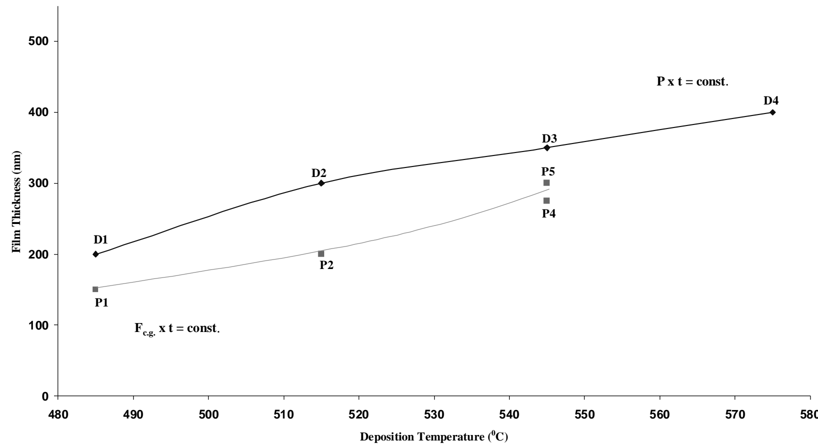

Fig. 7. Film thickness vs deposition temperature.

Table 3. Mean grain size, thickness and mean values of surface roughness.

Sample Name	*RMS values (nm)*	*Thickness (nm)*	*Mean grain size (nm)*
D1	26	200	24
D2	34	300	29
D3	60	350	35
D4	103	400	39
P1	11	150	17
P2	23	200	26
P3	45	250	28
P4	34	275	33
P5	29	300	34
P6	91	325	36

Among the films grown by the first method sample D4 presents the highest RMS value. Although the duration of deposition was the shortest one, the higher flowrate of the precursor led to a slightly rough surface.

Concerning RMS values for samples P1-P6, it can be concluded that the total flow of the precursor compared to the deposition temperature brings about dramatic results in the film quality with regards to its roughness. Through the comparison of RMS values of sample P3 with P2 and of sample P6 with samples P4 and P5, it can also be assumed that the total flow intensively affects the surface's smoothness, especially at high temperatures.

For both methods applied, the dependence of the film's surface roughness by the increase of deposition temperature is shown in Fig. 8. As can be observed, when air is used as the oxidizer the increase of the film's surface roughness at temperatures above 520 ^{o}C is by far steeper. This observation strengthens the assumption that crystal growth activates mainly at higher temperatures, if atmospheric air is used.

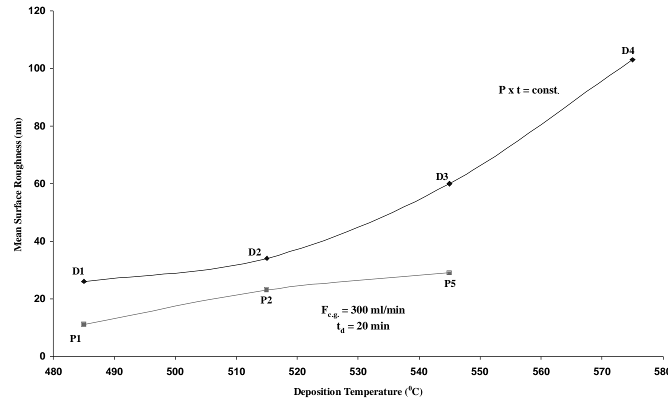

Fig. 8. Mean surface roughness vs deposition temperature.

3.4. Electrical properties

Table 4 summarizes the various resistivity values, at room temperature (ρ_{RT}), which were obtained by measuring the films' electrical resistance before and after annealing. Concerning the different resistivity values and their relation to film morphology for samples D1-D4, it can be said that the uniform surface (Fig. 4c) of sample D3 is probably responsible for its low value of ρ_{RT}. Among the rest of the films produced by the first method, sample D4 exhibits satisfying values of conductivity, even though they are lower than those of sample P3.

Table 4. Film resistivity values.

Sample	*ρ_{RT} (Ωcm) – as deposited*	*ρ_{RT} (Ωcm) – annealed*
D1	1.1	4.0×10^{-1}
D2	6.7×10^{-1}	9.4×10^{-2}
D3	7.1×10^{-2}	8.9×10^{-3}
D4	6.2×10^{-1}	9.3×10^{-2}
P1	5.5×10^{-1}	1.1×10^{-1}
P2	3.5×10^{-2}	6.4×10^{-3}
P3	5.8×10^{-3}	0.7×10^{-3}
P4	2.4×10^{-2}	4.6×10^{-3}
P5	1.8×10^{-2}	3.3×10^{-3}
P6	5.9×10^{-2}	8.0×10^{-3}

On the other hand, the porous microstructure of sample D2 renders high room temperature electrical resistivity ρ_{RT}. The maximum film resistivity was observed for sample D1. In this case, the thermal energy produced at 485 °C was insufficient to force the layer to grow completely.

Films D1-D4 exhibit lower conductivity values than films P1-P6 at the same deposition temperature. This could also, to some extent, be attributed to the presence of NaCl crystals, which are deposited through diffusion onto the matrix of films D1-D4. These crystals decrease the mobility of charge carriers [16]. The basic reason must be, however, the differences in film thickness. Samples D1-D4 are relatively thick and, as a result, the effect of grain scattering on conductivity is further intensified.

Among films derived from the second method, sample P3 exhibits the lowest resistivity value. It consists of uniform distribution of spherical grains, with relatively high density, thereby

minimizing the grain boundary scattering and inducing higher conductivity. Samples P2, P4 and P5 also present good uniformity and, as a result, exhibit low values of ρ_{RT}. Even if it was expected to have the lowest value of ρ_{RT} among the films deposited at 545 ^{o}C, sample P6 presents lower conductivity than that of samples P4 and P5. This must be due to the enhancement of oxidation phenomena. On the contrary, sample P1 presents the highest ρ_{RT}. In this case the low deposition temperature resulted in slower growth rate.

Through annealing in air, the electrical parameters for all films studied changed. The electrical resistivity decreased considerably. The improvement in film grain size by the heat treatment resulted in decrement of grain boundaries aiding in the movement of charge carriers. Higher conductivity was the general net consequence.

Deposition temperature dependence of electrical resistivity is another aspect worth exploring. Fig. 9 shows variation of ρ_{RT} before and after annealing versus deposition temperature for all thin layers. Regarding to films D1-D4 two distinct regions with inversed slopes can be observed, corresponding to a low temperature region (<545 ^{o}C) and to a high temperature region (>545 ^{o}C). From 515 ^{o}C the conductivity increases with increasing deposition temperature, with 545 ^{o}C being the maximum. By further increment of the deposition temperature the conductivity starts to decrease.

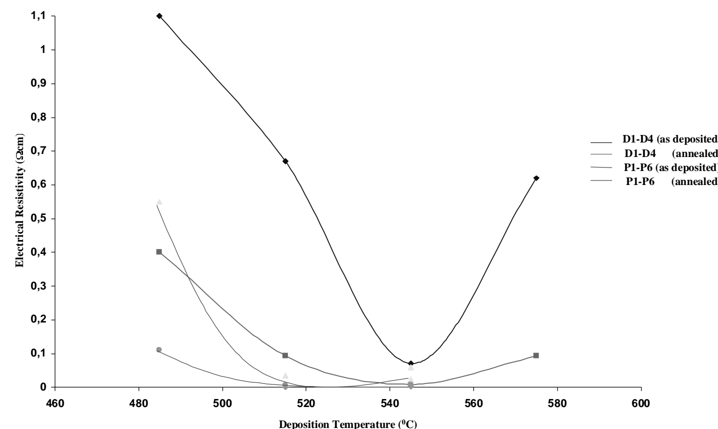

Fig. 9. Electrical resistivity vs deposition temperature. The points are experimental, whereas the lines are theoretical.

When films exhibit high crystallinity two mechanisms compete; the ordering of the structure and oxidation. While the ordering of the structure leads to a less resistant film, the oxidation draws the SnO_x near to its stoichiometric oxide, i.e. diminishes film defects, which are responsible for the conductivity [6, 18]. It should be noted that during the cooling process the samples were further oxidized, thus eliminating oxygen vacancies, which act as electron donors in SnO_2 films introducing states within the energy gap. The higher the deposition temperature, the longer the time to cool down. As a result, oxidation phenomena become enhanced at elevating deposition temperatures and this is why the film's resistance increases. The above are clear especially in the case of sample D4.

With regards to samples P1-P6 the maximum conductivity is observed at temperatures around 515 ^{o}C (Fig. 9). Since pure oxygen was used as the oxidizer, the oxidation process seemed to have been completed more easily, i.e. at relatively lower deposition temperatures. At 515 ^{o}C, grain scattering of interstitial defects, which depends significantly upon film thickness is stabilized and compensates the carrier's scattering at characteristic centres, which, is in turn attributed to ionised impurities. At deposition temperatures different to 515 ^{o}C, one of the previous mentioned mechanisms of electrical resistance, dominates the other.

As was previously mentioned, at relatively low temperatures films can not fully grow when air is used as the oxidizer. In this case they present some amount of amorphous structure, which induces higher resistivity. However, they can present sufficient conductivity. The reason is that the % wt concentration of oxygen in the air is low. As a result the SnO_x produced films with air functioning as the oxidizer are kept far from their exact stoichiometry. The assumption that the oxidation process is of great importance can be well proved by the observation that samples P1-P6 presented slight variations in film resistivity values across the substrate's surface. This should be attributed to tiny variations in films' oxygen concentration.

Electrical resistivity measurements have been also performed in the temperature range from 25 to 250 ^oC (Fig. 10-11). These resistivity values were obtained for all films after annealing. It is obvious that through the increase of temperature the electrical resistivity decreases at an exponential rate. The reason is that, at high temperatures the mechanism of impurities' thermal activation becomes the dominant one. The concentration of charge carriers increases and, as a result, film resistivity decreases.

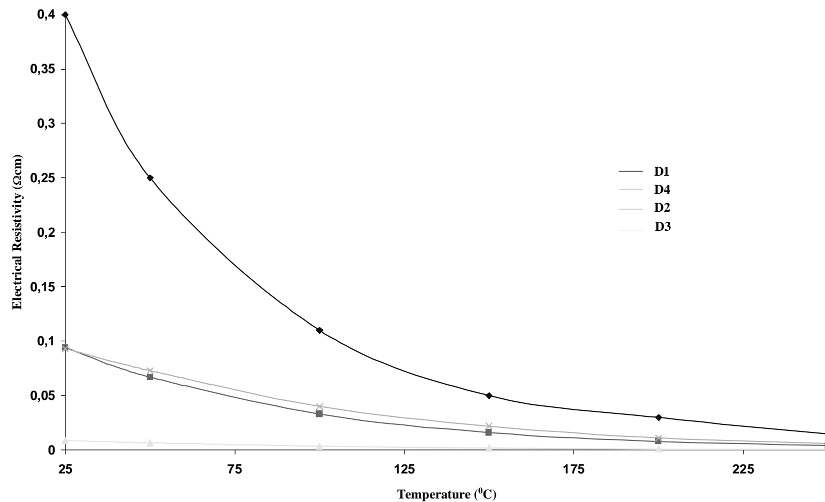

Fig. 10. Electrical resistivity vs temperature (Samples D1-D4).

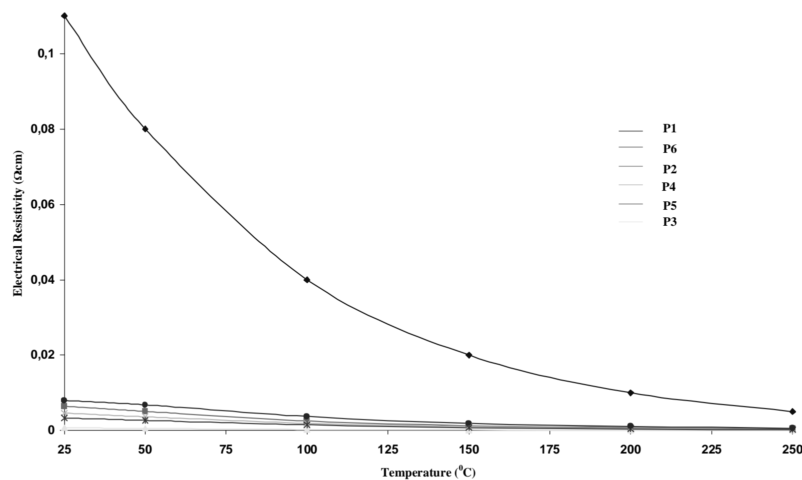

Fig. 11. Electrical resistivity vs temperature (Samples P1-P6).

However, in the case of samples D1-D4 the decrement in electrical resistivity is slightly faster than that of samples P1-P6, when produced at the same deposition temperature. This could be attributed to the fact that oxidation of samples D1-D4 proceeds at a slower pace. As a result the oxygen vacancies, which are responsible for conductivity, multiply in films grown by the use of air as the oxidizer. What is more, at elevating temperatures the concentration of charge carriers seems to increase more easily.

4. Conclusions

As was demonstrated, the low – cost CVD technique, described in this study, can be used to obtain uniform conductive layers of SnO_2, with good repeatability. By comparing the two methods used the following noteworthy conclusions have been reached:

- All films were polycrystalline with cassiterite structure. Temperature influences crystallinity more powerfully than deposition duration. Films exhibited higher crystallinity when air rather than pure oxygen was used as the oxidizer.
- Annealing in air improves the crystallinity, inducing the films higher conductivity, since the grain boundaries occupy a smaller part of the film volume. Especially, when pure oxygen is used as the oxidizer annealing is of major importance.
- Higher deposition temperature and longer process duration (or higher precursor's flow) lead to increment of film thickness and mean grain size, which, in turn, increase surface roughness. When pure oxygen is used as the oxidizer films present a quite smooth surface. On the other hand, films grown with air functioning as the oxidizer present a relatively rough surface, since the % w.t. oxygen concentration in the air is low and increased precursor's flows are needed.
- The mean surface roughness is affected mostly by the total precursor's flow when pure oxygen is used. When the oxidizer is air, surface roughness is significantly affected by deposition temperature and increases rapidly above 520 ^{o}C.
- Uncommon morphologies, such as dendrites, can occur at relatively high temperatures, together with the presence of NaCl crystals.
- When air is used as the oxidizer, deposition takes place more easily at high temperatures. However, in this case oxidation phenomena diminish most of the defects responsible for conductivity and film resistivity increases. When pure oxygen is used as the oxidizer, the oxidation process seems to complete more easily, i.e. at lower deposition temperatures. Films of high conductivity can be obtained in the first method at temperatures around 545 ^{o}C, whereas in the second method at temperatures between 515 and 545 ^{o}C.
- At relatively low temperatures films can not completely grow when air is used as the oxidizer. In this case they present lower crystallinity, which induces higher resistivity. However, they can present sufficient conductivity, since the % wt concentration of oxygen in the air is low and the SnO_x produced films are kept far from their exact stoichiometry.

Acknowledgements

The authors would like to express their gratitude to Professor J.N. Avaritsiotis, School of Electrical and Computer Engineering, National Technical University of Athens, for his most helpful guidance concerning the CVD manufacturing and the thin film development.

References

[1] E. Elangovan, M. P. Singh, M. S. Dharmaprakash, K. Ramamurthi, J. Optoelectron. Adv. Mater. **6**(1), 197 (2004).
[2] V. Brinzari, G. Korotcenkov, J. Schwank, Y. Boris, J. Optoelectron. Adv. Mater. **4**(1), 147 (2002).
[3] E. Elangovan, K. Ramamurthi, J. Optoelectron. Adv. Mater. **5**(2), 415 (2003).
[4] K. Papadopoulos, J. N. Avaritsiotis, Sensors and Actuators B: Chemical **28**(3), 201 (1995).
[5] K. Papadopoulos, D. S. Vlachos, J. N. Avaritsiotis, Sensors and Actuators B: Chemical **32**(1), 61 (1996).
[6] Roy Gordon, Journal of Non Crystalline Solids, **218**(3), 81 (1997).
[7] A. Bouteville, J. Optoelectron. Adv. Mater. **7**(2), 599 (2005).
[8] E. Elangovan, K. Ramamurthi, J. Optoelectron. Adv. Mater. **5**(1), 45 (2003).
[9] V. Craciun, D. Craciun, X. Wang, T. J. Anderson, R. K. Singh, J. Optoelectron. Adv. Mater. **5**(2), 401 (2003).
[10] J. Touskova, J. Kovanda, L. Dobiasova, V. Parizek, P. Kielar, Solar Energy Materials and Solar Cells **37**(3-4), 357 (1995).
[11] K. L. Choy, Progress in Materials Science **48**(2), 57 (2003).
[12] H. Kobayashi, Y. Uebou, T. Ishida, S. Tamura, S. Mocluzuki, T. Mihara, M. Tabuchi, H. Kageyama, Y. Yamamoto, Journal of Power Sources **97-98**, 229 (2001).
[13] G. S. Park, G. M. Yang, Thin Solid Films, **365**(1), 7 (2000).
[14] J. Szanyi, Applied Surface Science, **185**(3-4), 161 (2002).
[15] D. Davazoglou, Thin Solid Films, 302(1-2), 204 (1997).
[16] J. L. Van Heerden, R. Swanepoel, Thin Solid Films, **299**(1-2), 72 (1997).
[17] G. Lucovsky, D.V. Tsu, In: 'Thin film processes- Volume I', eds: J.L. Vossen, W. Kern, Boston Academic Press, 565, (1991).
[18] C. F. Wan, R. D Mc Grath, W. F. Keenan, S. N. Franck, J. Electrochem. Soc. **136**(5), 1459 (1989).